Electrochemical Characterization and Theoretical Insight of A Series of 2D MOFs, $[M(bipy)(C_4O_4)(H_2O)_2]\cdot 3H_2O$ (M = Mn (1), Fe (2), Co (3) and Zn (4)) for Chemical Sensing Applications

Yi-Ting Hsieh,* Ssu-Chia Huang, Shih-I Lu,* Hsiao-Hsun Wang, Tsai-Wen Chang, and Chih-Chieh Wang*, Gene-Hsiang Lee,[b] and Yu-Chun Chuang,[c]

[a]Department of Chemistry, Soochow University. Taipei City, 111, Taiwan.

[b]Instrumentation Center, National Taiwan University, Taipei, 10617, Taiwan.

[c]National Synchrotron Radiation Research Center, Hsinchu, 30076, Taiwan.

Support Information

Table S1. Experimental data of CV measurements of as-prepared electrodes in 0.5 mM NFZ/0.1 M PB solution (pH = 7) with a scan rate of 50 mV s^{-1}

Electrode	Peak potential (V)	Maximum peak current density (mA cm^{-2})
Bare SPCE	-0.49805	0.37
Mn-MOF/SPCE	-0.49316	0.79
Fe-MOF/SPCE	-0.50049	0.65
Co-MOF/SPCE	-0.47852	0.63
Zn-MOF/SPCE	-0.55908	0.39

Table S2. HSE06/DZP//Expt calculated band gap of the MOF of study and the spin polarization of metal ion within the MOF environment and in the free ion state (in italics)

Metal ion	Band Gap of MOF (eV)	Spin polarization of metal ion
Mn(II)	1.834	4.627; *5*
Fe(II)	1.841	3.705; *4*
Co(II)	2.167	2.720; *3*
Zn(II)	2.266	0.000; *0*

Table S3. Comparison of the Mn-MOF modified SPCE with other modified electrodes for the quantitative analysis of NFZ.

Working electrode	Method	Potential (V vs Ag/AgCl)	Linear range (μM)	Detection limit (μM)	Ref.
Au-AuNR[a]	Chronoamperometry	-0.4	50-610	6.51	[1]
Gr/Fe3O4/GCE[b]	Chronoamperometry	-0.395	10-109	2.92	[2]
MWCNTs-COOH/GCE[c]	Chronoamperometry	-0.36	5-1090	0.224	[3]
S/M*/PME[d]	DPV	-0.1 to -0.6	0.05-2.0	0.012	[4]
PACBK/GCE[e]	DPV	0 to -0.7	0.2-15.0; 15.0-80.0	0.028	[5]
AuNPs/Gr/TFGE[f]	DPV	0 to -0.8	0.2-4800	0.13	[6]
Hollow MIL-101/GCE[g]	DPV	0.6 to1.4	0.030-55	0.01	[7]
DUT-67/T-PPY-2/GCE[h]	DPV	-0.1 to -0.7	9.08-354.08; 354.08-1004.4	8.7	[8]
BC/Cr2O3/Ag/MIP/GCE[i]	DPV	-0.2 to -0.7	0.005-10	0.003	[9]
Mn-MOF/SPCE	DPV	0 to -0.7	32.65-751.55	21.08	this work

a : gold nanorods electrodeposited-Au electrode

b : graphene and Fe_3O_4 nanoparticles modified glassy carbon electrode

c: carboxylic multi-walled carbon nanotubes modified glassy carbon electrode

d: screen-printed carbon electrode coated electrochemically activated MWCNT (M*) and covered PME

e: poly(acid chrome blue K)-modified glassy carbon electrode

f: gold nanoparticles/graphene modified thin film gold electrode

g: MIL-101 modified glassy carbon electrode

h: DUT-67 combines tubular polypyrrole modified glassy carbon electrode

i: a molecularly imprinted polymer coating biomass carbon decorated with MOF-derived Cr_2O_3 and silver nanoparticles

Spearman correlation coefficient:

The Spearman correlation coefficient is defined as the Pearson correlation coefficient between the rank variables. The Spearman correlation coefficient, ρ, is calculated by

$$\rho = 1 - \frac{6\sum_i d_i^2}{n(n^2-1)}$$

in which, n is the number of data points and d_i is the difference in ranks of the i^{th} data point.

Table S4. Crystal data and structural refinement for Co-MOF.

Formula	$C_{14}H_{18}Co_1N_2O_9$	Fw	417.23
cryst syst	monoclinic	space group	$P\ 2_1/c$
a (Å)	18.8828(7)	α (deg)	90.0
b (Å)	11.3176(4)	β (deg)	94.0405(14)
c (Å)	8.0387(3)	γ (deg)	90.0
V (Å^3)	1713.66(11)	Z	4
D_{calc} (g/cm^3)	1.617	μ (mm^{-1})	1.054
F(000)	860	max and min trans	0.6515, 0.7459
reflns collected	4887	unique reflns (I > 2σ(I))	4632
R_1, wR_2[a] (I > 2σ(I))	0.0710, 0.1311	R_1, wR_2[a] (all data)	0.0753, 0.1329
GOF on F^2	1.306	no. of variable	269

[a]$R_1 = \Sigma||F_o - F_c||/\Sigma|F_o|$; $wR_2 = [\Sigma w|F_o^2 - F_c^2|^2/\Sigma w(F_o^4)]^{1/2}$.

Table S5. Selected bond lengths (Å) and angle (°) for Co-MOF [a]

Co(1)–O(5)	2.035(3)	Co(2)–O(6)	2.062(3)
Co(1)–O(5)$_i$	2.035(3)	Co(2)–O(6)$_{ii}$	2.062(3)
Co(1)–O(1)	2.102(3)	Co(2)–O(3)	2.126(3)
Co(1)–O(1)$_i$	2.102(3)	Co(2)–O(3)$_{ii}$	2.126(3)
Co(1)–N(1)	2.225(3)	Co(2)–N(2)	2.126(3)
Co(1)–N(1)$_i$	2.225(3)	Co(2)–N(2)$_{ii}$	2.126(3)
O(5)–Co(1)–O(5)$_i$	180.0	O(6)$_{ii}$–Co(1)–O(6)	180.0
O(5)$_i$–Co(1)–O(1)	85.80(12)	O(6)$_{ii}$–Co(1)–O(3)$_{ii}$	92.28(12)
O(5)$_i$–Co(1)–O(1)$_i$	94.20(12)	O(6)–Co(1)–O(3)$_{ii}$	87.73(12)
O(5)–Co(1)–O(1)	94.20(12)	O(6)$_{ii}$–Co(1)–O(3)	87.73(12)
O(5)$_i$–Co(1)–O(1)	85.80(12)	O(6)–Co(1)–O(3)	92.28(12)
O(1)$_i$–Co(1)–O(1)	180.00(6)	O(3)$_{ii}$–Co(1)–O(3)	180.00(6)
O(5)–Co(1)–N(1)$_i$	89.51(13)	O(6)$_{ii}$–Co(1)–N(2)$_{ii}$	88.31(13)
O(5)$_i$–Co(1)–N(1)$_i$	90.48(13)	O(6)–Co(1)–N(2)$_{ii}$	91.69(13)
O(1)$_i$–Co(1)–N(1)$_i$	93.30(12)	O(3)$_{ii}$–Co(1)–N(2)$_{ii}$	86.27(12)
O(1)–Co(1)–N(1)$_i$	86.70(12)	O(3)–Co(1)–N(2)$_{ii}$	93.73(12)
O(5)–Co(1)–N(1)	90.48(13)	O(6)$_{ii}$–Co(1)–N(2)	91.69(13)
O(5)$_i$–Co(1)–N(1)	89.51(13)	O(6)–Co(1)–N(2)	88.31(13)
O(1)$_i$–Co(1)–N(1)	86.70(12)	O(3)$_{ii}$–Co(1)–N(2)	93.73(12)
O(1)–Co(1)–N(1)	93.30(12)	O(3)–Co(1)–N(2)	86.27(12)
N(1)$_i$–Co(1)–N(1)	180.00(6)	N(2)$_{ii}$–Co(1)–N(2)	180.00(6)

[a] Symmetry transformations used to generate equivalent atoms: $i = -x + 2, -y + 3, -z + 1$; $ii = -x + 1, -y + 2, -z$.

Table S6. The O–H···O hydrogen bonds for Co-MOF.[a]

D–H···A	D–H (Å)	H···A (Å)	D···A (Å)	∠ D–H···A (°)
O(5)–H(5A)···O(2)$_{i}$	0.825	1.887	2.701	168.7
O(5)–H(5B)···O(2)$_{ii}$	0.824	1.812	2.607	161.8
O(6)–H(6A)···O(4)$_{iii}$	0.830	1.927	2.735	164.0
O(6)–H(6B)···O(4)$_{iv}$	0.830	1.826	2.641	166.8
O(7)–H(7A)···O(3)$_{iii}$	0.828	2.047	2.858	166.4
O(7)–H(7B)···O(8)$_{v}$	0.826	1.950	2.752	163.6
O(8)–H(8A)···O(9)	0.829	1.958	2.760	162.7
O(8)–H(8B)···O(7)	0.831	1.967	2.761	159.6
O(9)–H(9A)···O(1)$_{vi}$	0.828	2.036	2.837	162.3
O(9)–H(9B)···O(8)$_{v}$	0.827	2.042	2.783	149.0

[a] Symmetry transformations used to generate equivalent atoms: *i* = −*x* + 2, −*y* − 1, −*z* + 1; *ii* = −*x* + 2, −*y* + 7/2, −*z* + 5/2; *iii* = −*x* + 1, −*y* − 1, −*z*; *iv* = −*x* + 1, −*y* + 5/2, −*z* + 3/2; *v* = *x*, −*y* + 3/2, *z* + 1/2; *vi* = *x*, −*y* + 5/2, *z* − 1/2.

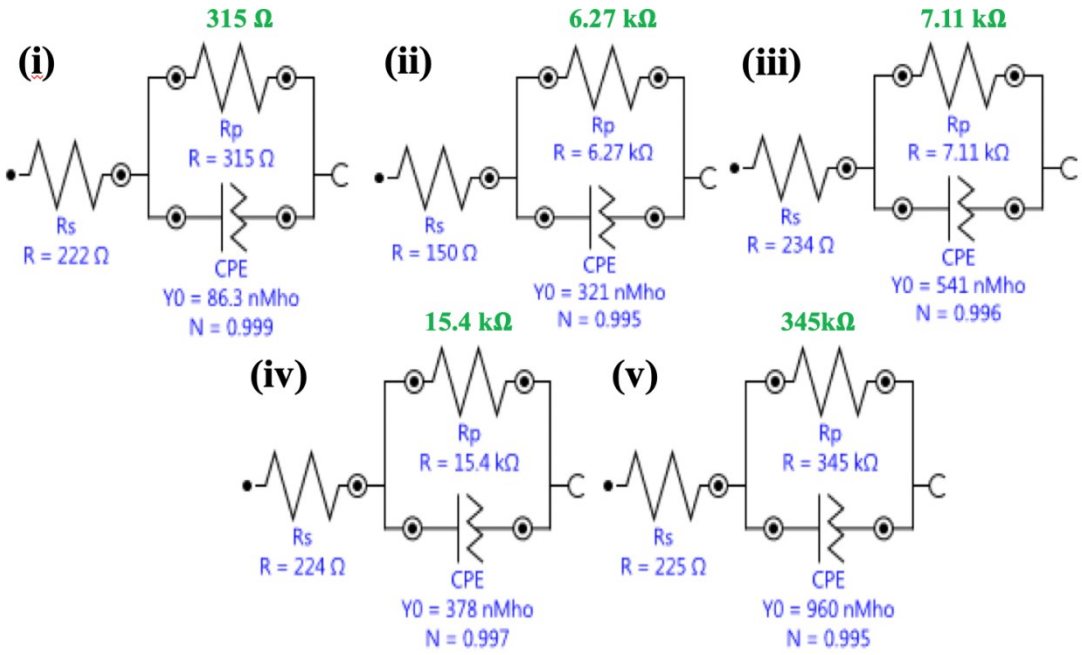

Figure S1. Related equivalent circuit of the as-prepared MOF modified electrodes in a solution of 5 mM $[Fe(CN)_6]^{3-/4-}$ with 0.1 M KCl. (i) bare SPCE, (ii) Mn-MOF, (iii) Fe-MOF, (iv) Co-MOF, and (v) Zn-MOF.

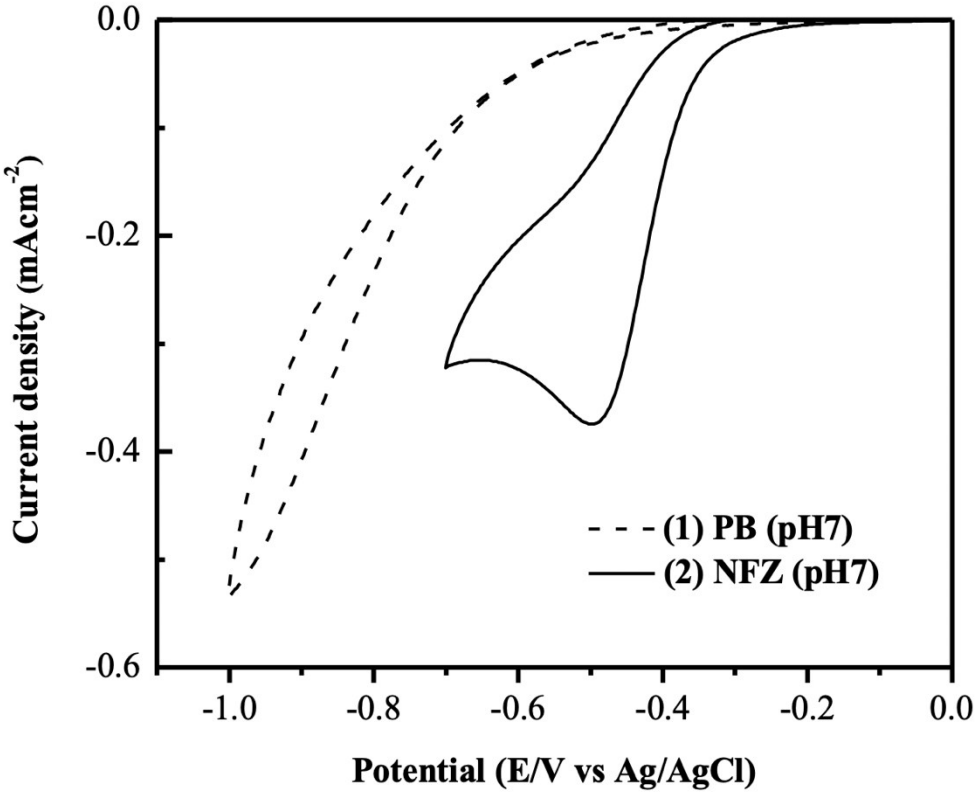

Figure S2. CV curves recorded on the SPCE in 0.1M PB solution (pH 7) (a) without and (b) with 0.5 mM NFZ. The scan rate is 50 mV s^{-1}.

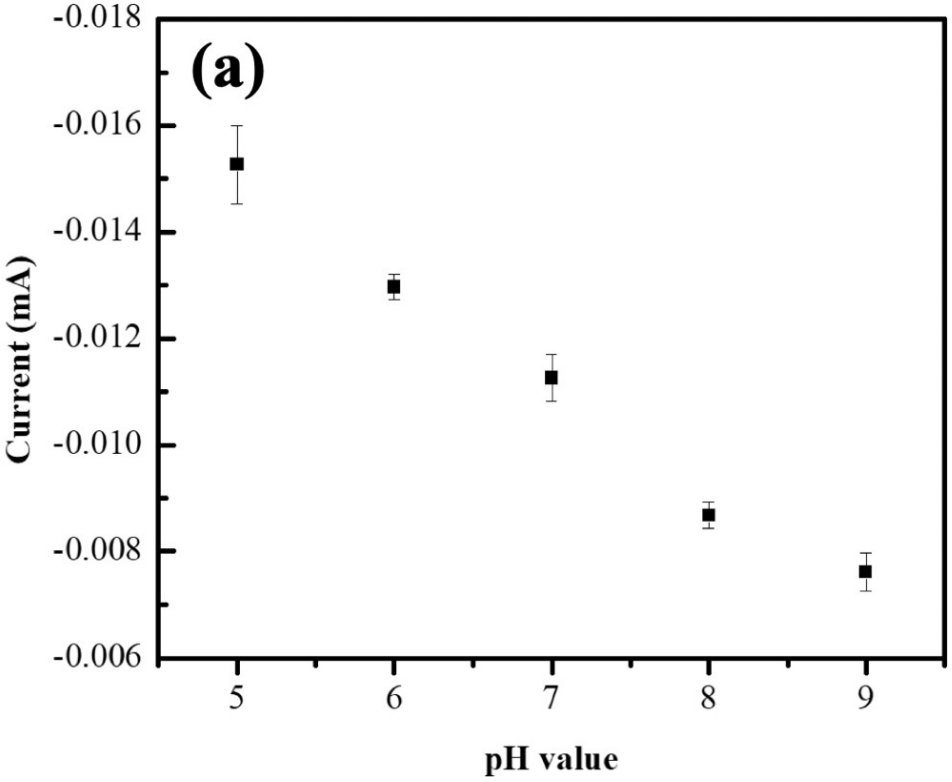
(a)
Current (mA)
-0.018
-0.016
-0.014
-0.012
-0.010
-0.008
-0.006
5
6
7
8
9
pH value

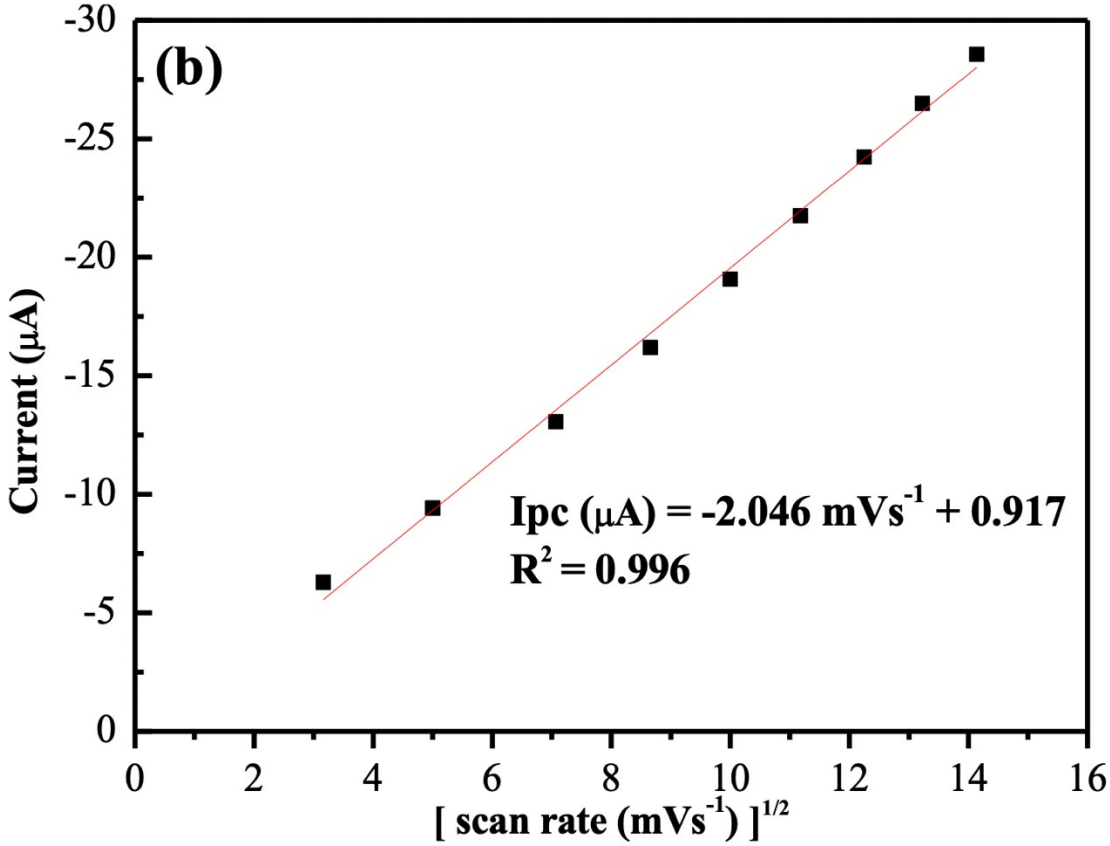
(b)
Current (μA)
-30
-25
-20
-15
-10
-5
0
0
2
4
6
8
10
12
14
16
[scan rate (mVs-1)]1/2
Ipc (μA) = -2.046 mVs-1 + 0.917
R2 = 0.996

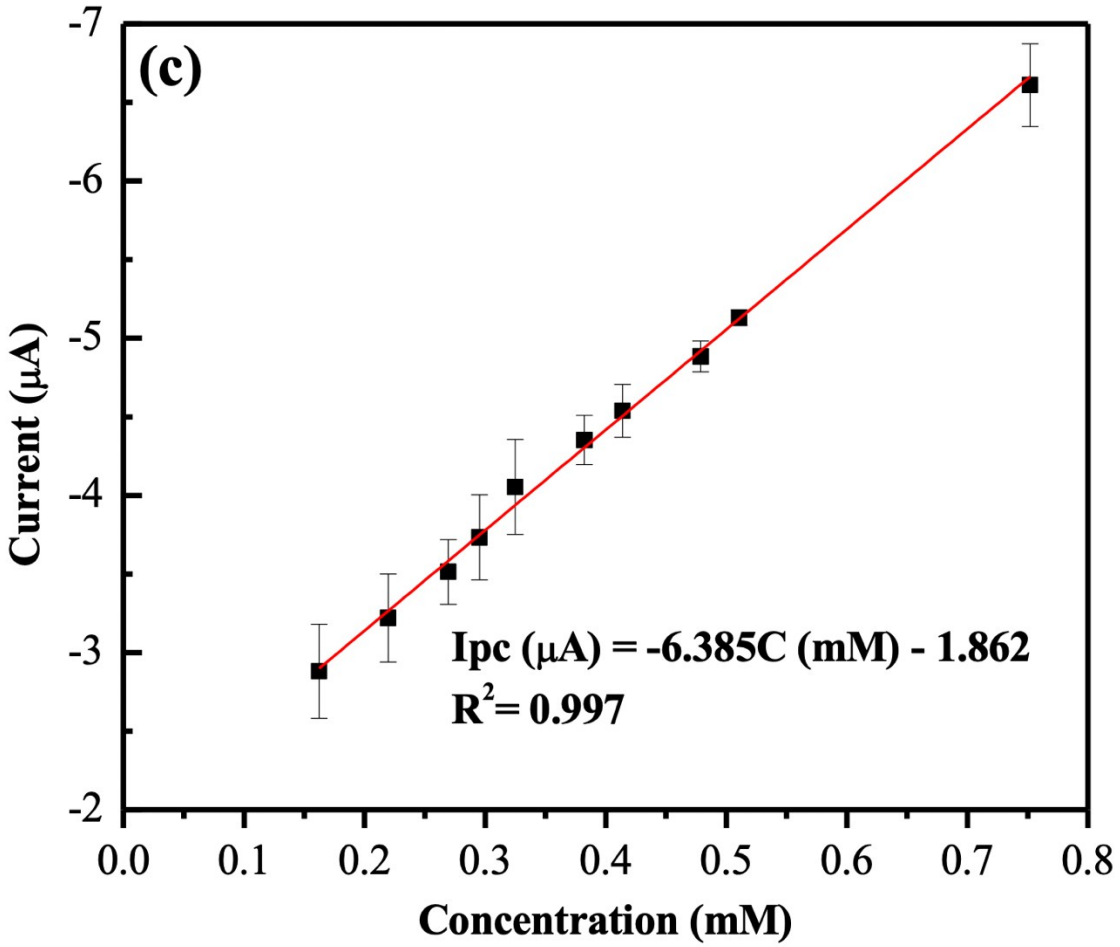

Figure S3. (a) Plot of peak current vs. pH value. The current responses were obtained by 5 replicate measurements using 5 modified electrodes. The results were obtained from cyclic voltammograms of 0.5 mM NFZ in 0.1M PB solution on Mn-MOF modified electrode. (b) The plot of the peak current (μA) vs the square root of the scan rate (10−200 mV s^{-1}), and (c) linear fitting between the current peak (μA) and the corresponding concentration (mM) recorded on Mn-MOF modified electrode in 0.5 mM NFZ in PB solution (pH 5). The current responses were obtained by 5 replicate measurements using 5 modified electrodes.

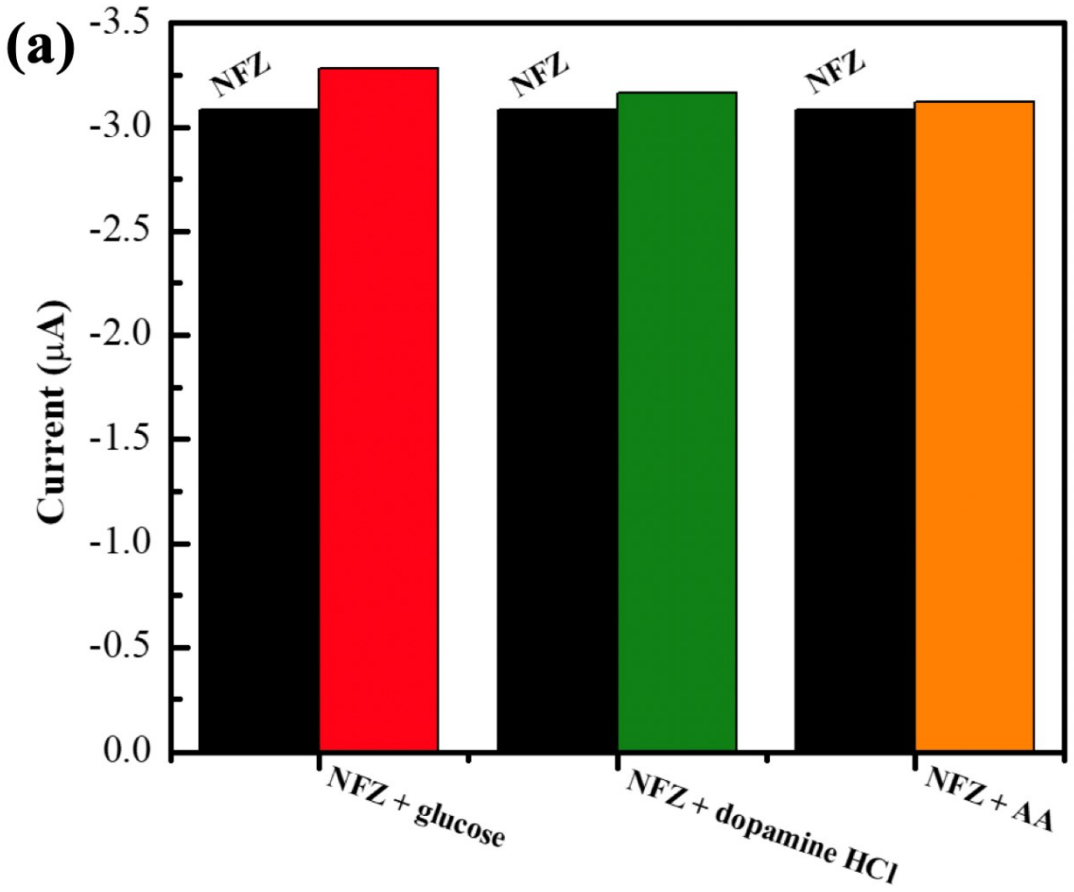
(a)
Current (μA)
-3.5
-3.0
-2.5
-2.0
-1.5
-1.0
-0.5
0.0
NFZ
NFZ
NFZ
NFZ + glucose
NFZ + dopamine HCl
NFZ + AA

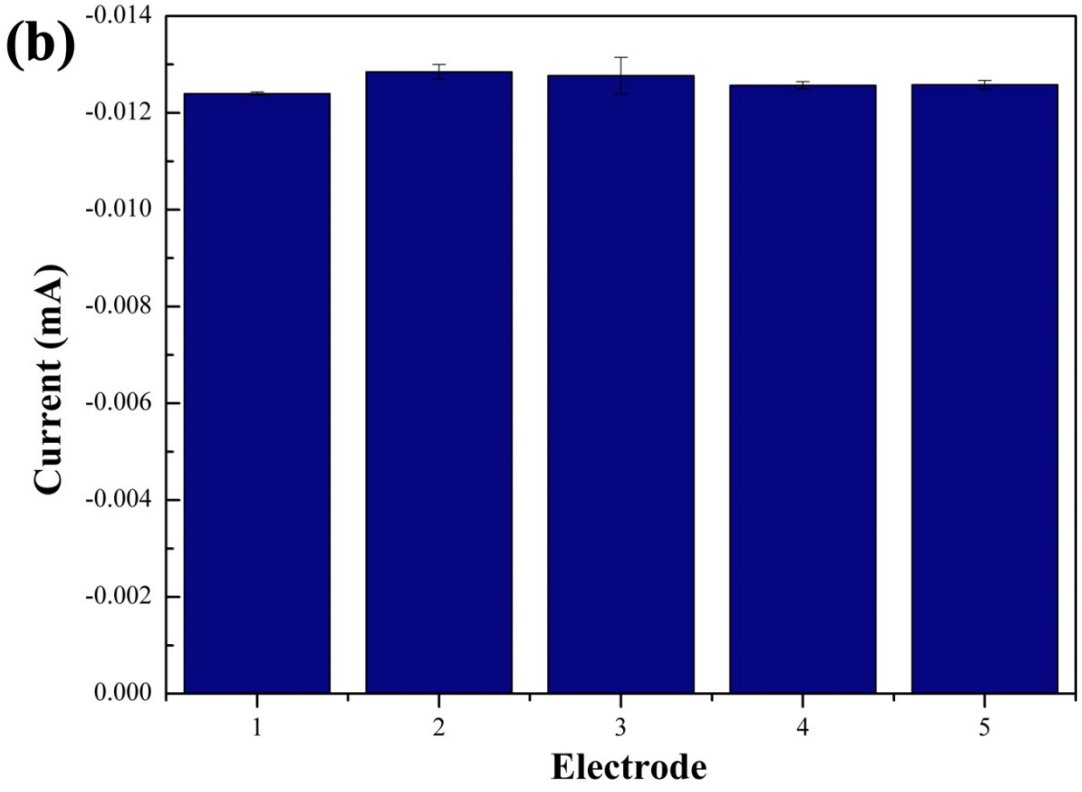
(b)
Current (mA)
-0.014
-0.012
-0.010
-0.008
-0.006
-0.004
-0.002
0.000
1
2
3
4
5
Electrode

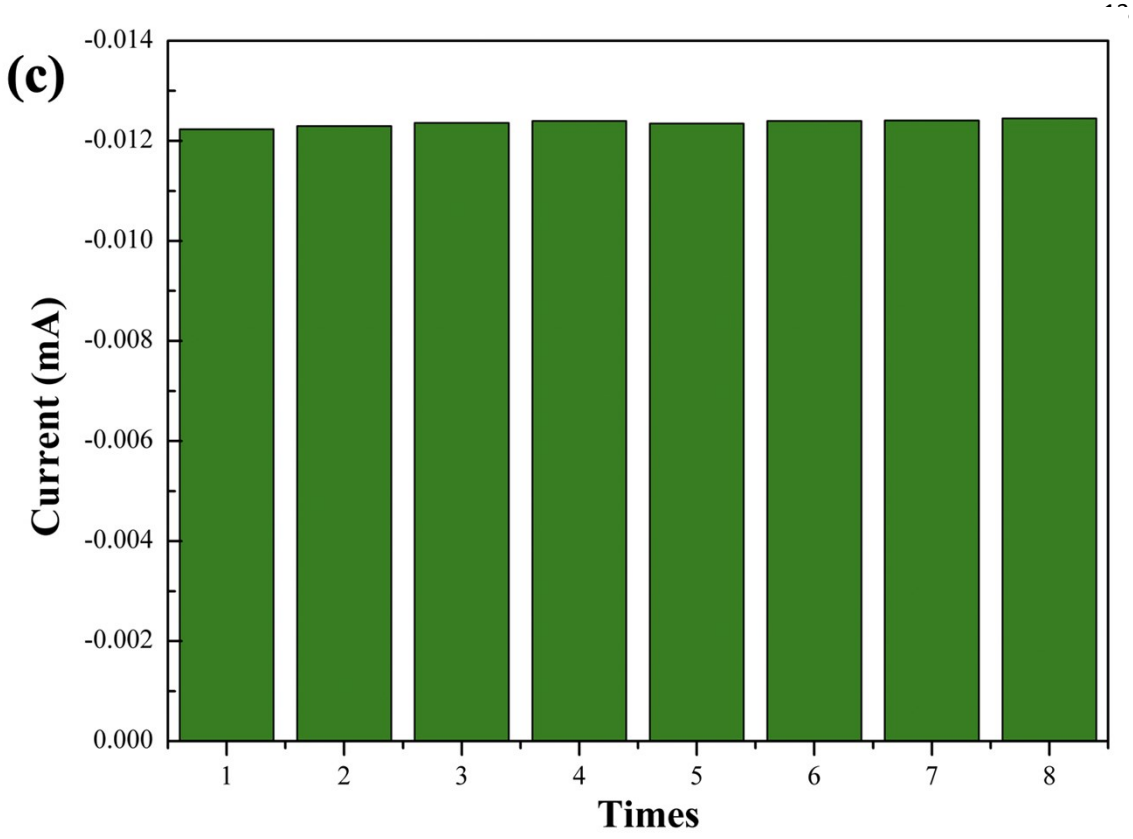

Figure S4. The evaluation of Mn-MOF modified electrode for (a) selectivity in presence of common interferents and the concentration of each interferents is 5mM, (b) the reproducibility and (c) the repeatability of 0.5 mM NFZ in PB solution (pH 5).

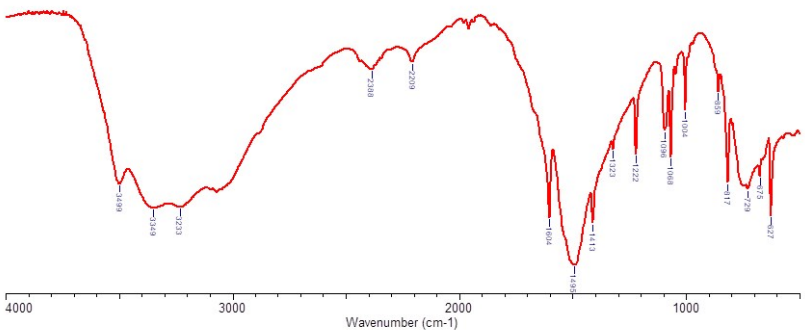
3499
3349
3233
2380
2239
1604
1498
1413
1323
1222
1086
1068
1004
939
817
729
675
627
4000
3000
2000
1000
Wavenumber (cm-1)

(a)

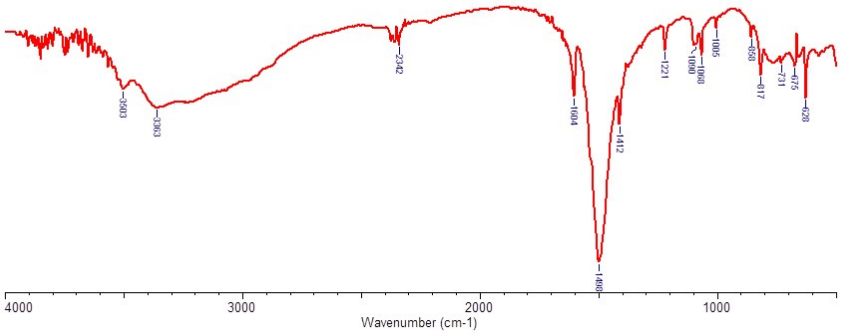
3503
3363
2342
1604
1498
1412
1221
1090
1068
1005
938
817
731
675
628
4000
3000
2000
1000
Wavenumber (cm-1)

(b)

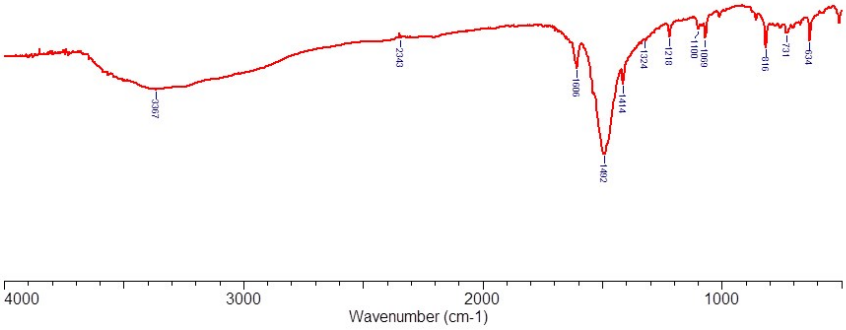
3367
2343
1696
1492
1414
1324
1218
1100
1069
1016
731
634
4000
3000
2000
1000
Wavenumber (cm-1)

(c)

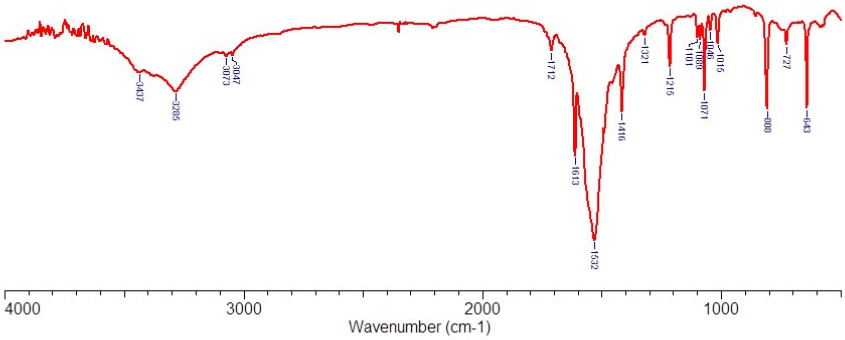
3437
3285
2947
2873
1712
1613
1532
1416
1321
1216
1101
1069
1046
1015
1071
727
688
643
4000
3000
2000
1000
Wavenumber (cm-1)

(d)

Figure S5. IR spectra of (a) Mn-MOF, (b) Fe-MOF, (c) Co-MOF, (d) Zn-MOF.

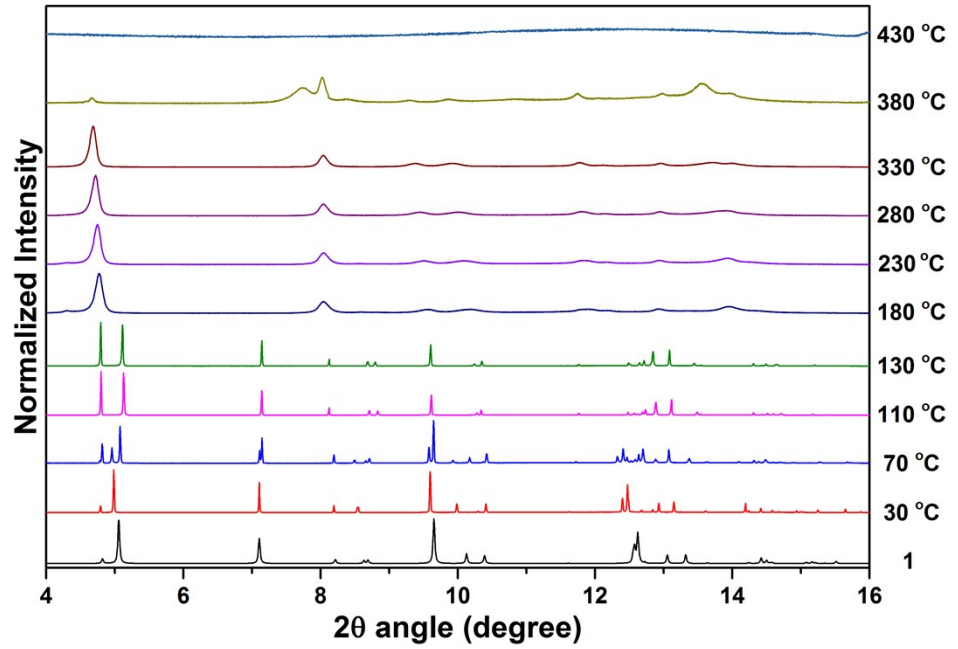

(a)

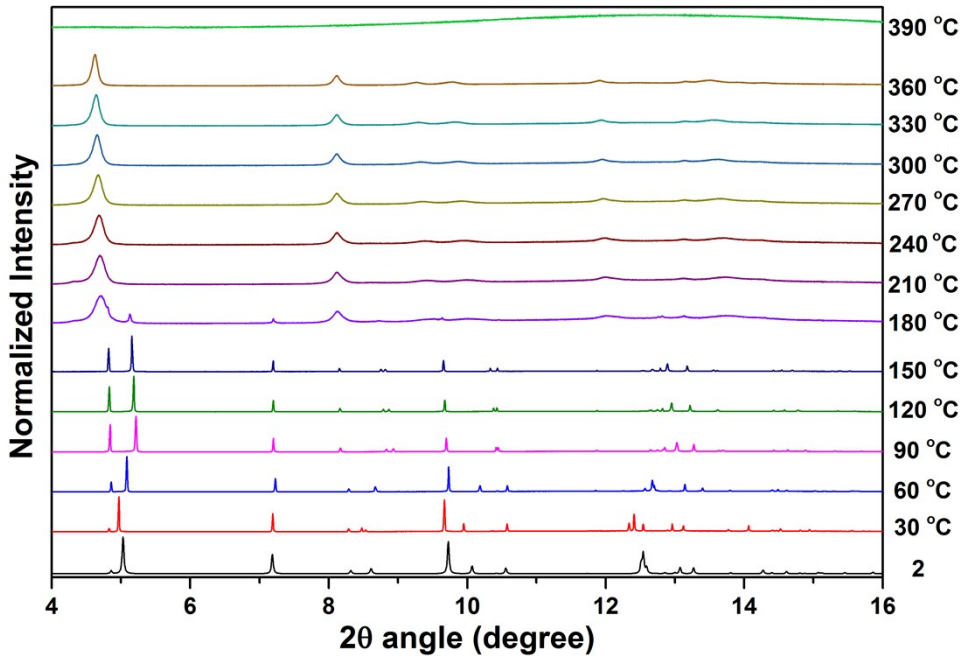

(b)

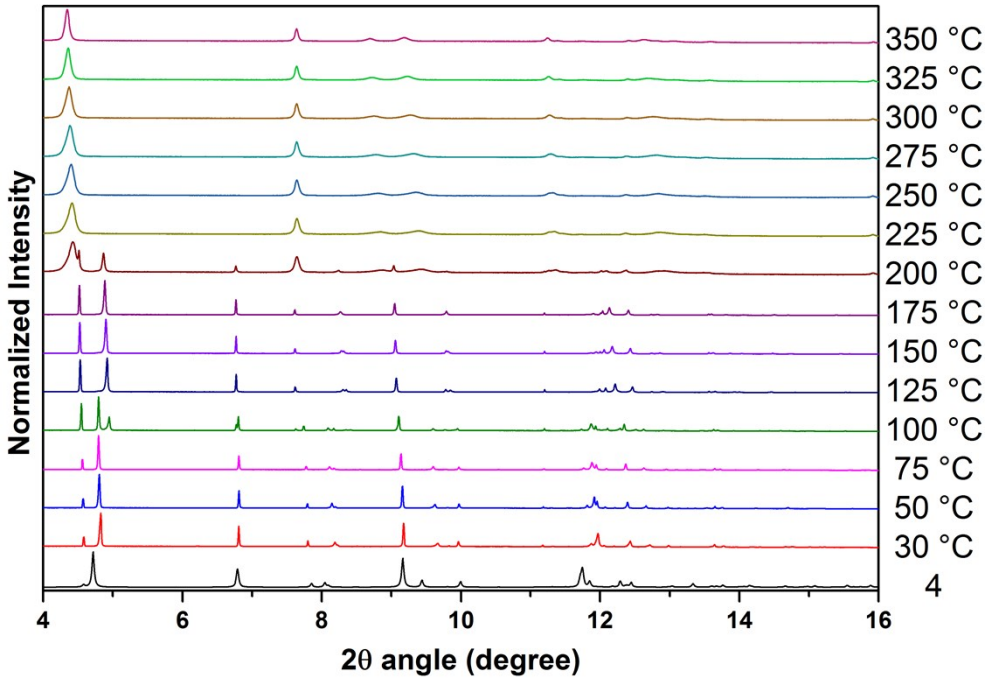

(c)

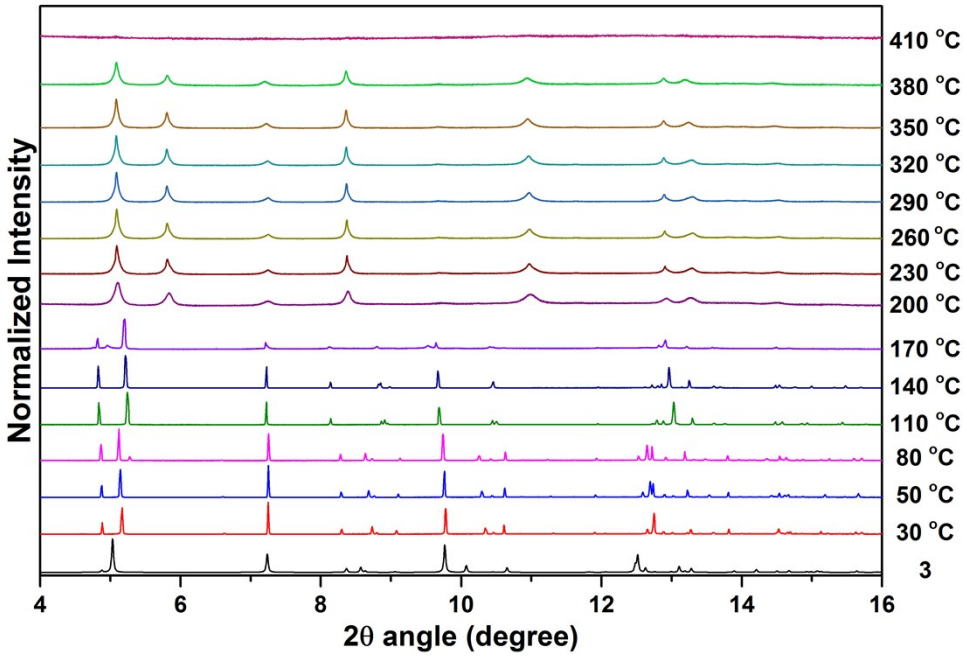

(d)

Figure S6 Temperature-dependent PXRD measurements of (a) Mn-MOF, (b) Fe-MOF, (c) Co-MOF, (d) Zn-MOF.

References

1. A. Rahi, N. Sattarahmady, R. Dehdari Vais, H. Heli, *Sensors and Actuators B: Chemical.* 2015**, 210**, 96-102.
2. B. He, G. Du, *International Journal of Electrochemical Science.* 2016**,** 8546-8560.
3. B. He, M. Li, *International Journal of Electrochemical Science.* 2018**,** 4174-4181.
4. S.-H. Chiu, Y.-L. Su, Anh V. T. Le, S.-H. Cheng, *Analytical and Bioanalytical Chemistry.* 2018**, 410**, 6573-6583.
5. C. Chen, W. Chen, J. Jiang, L. Qian, F. Qiu, *International Journal of Environmental Analytical Chemistry.* 2019**,** 1099-1115.
6. B. He, H. Liu, *Microchemical Journal.* 2019**, 150**, 104108.
7. T. Gan, J. Li, L. Xu, Y. Yao, Y. Liu, *Journal of Electroanalytical Chem.* 2019**, 848**, 113287.
8. H. Wang, X. Bo, M. Zhou, L. Guo, *Analytica Chimica Acta.* 2020**, *1109***, 1-8.
9. J. Cheng, Y. Li, J. Zhong, Z. Lu, G. Wang, M. Sun, Y. Jiang, P. Zou, X. Wang, Q. Zhao, Y. Wang, H. Rao, *Chemical Engineering Journal.* 2020**, 398**, 125664.